Scanning Electron Microscopy

Volume 1986 | Number 4 Article 31

10-1-1986

Scanning Electron Microscopy in Bone Pathology: Review of Methods, Potential and Applications

A. Boyde
University College London

E. Maconnachie
University College London

S. A. Reid
University College London

G. Delling
Universität Hamburg

G. R. Mundy
University of Texas

SCANNING ELECTRON MICROSCOPY/1986/IV (Pages 1537-1554)
SEM Inc., AMF O'Hare (Chicago), IL 60666-0507 USA

0586-5581/86$1.00+05

SCANNING ELECTRON MICROSCOPY IN BONE PATHOLOGY: REVIEW OF METHODS, POTENTIAL AND APPLICATIONS

A. Boyde*, E. Maconnachie, S. A. Reid, G. Delling[1] and G. R. Mundy[2]

Department of Anatomy and Embryology, University College London, London WC1E 6BT, UK
[1]Institut für Pathologie, Universität Hamburg, 2000 Hamburg 20, West Germany
[2]Department of Medicine/Endocrinology, University of Texas, Health Sciences Center San Antonio, TX 78284 USA

(Received for publication May 09, 1986, and in revised form October 01, 1986)

Abstract

This article reviews the applications of SEM methods to human bone pathologies referring to studies made at UCL. We consider the methods which may be most suitable; these prove to be not "routine" in the context of most bio-medical applications of SEM.

Valuable information can be obtained from a bone sample if its edges are ground flat, before making either (a) a matrix surface preparation by washing away all the cells or (b) a mineralising front preparation, by also dissolving the osteoid - for which hydrogen peroxide is recommended to produce a robust specimen. BSE contrast from a cut block surface can be used to measure bone phase volume. SE contrasts from natural surfaces (trabeculae, canals and lacunae) can be used to study forming, resting and resorbing* surfaces both qualitatively and quantitatively (* except in the case of histological osteomalacia, where the existence of osteoid will go undetected and reversal lines will be difficult to distinguish from recently resorbed surfaces).

We also recommend the use of PMMA embedded bone blocks, which can be used as obtained from the pathologist, but are better embedded by a more rigorous procedure. BSE image analysis can be used to quantitate bone density fractions opening up a completely new investigative method for the future. Osteoid can be measured automatically using CL if the bone sample is block stained with brilliant sulphaflavine before embedding or if a scintillant is added to the embeddant. We give examples of observations made from a number of bone diseases: vitamin D resistant rickets, ostegenesis imperfecta; osteomalacia; osteoporosis; hyperparathyroidism; fluorosis; Paget's disease; tumour metastasis to bone.

KEYWORDS: Human bone disease; block face microscopy; tandem scanning reflected light microscopy; image analysis.

***Address for correspondence:** Alan Boyde
Department of Anatomy and Embryology,
University College London, Gower Street,
London WC1E 6BT, United Kingdom
Phone:(UK=44) (1) 387 7050 Ext. 3316

Introduction

Why SEM?

SEM is obviously an appealing way of looking at skeletal tissues [19, 23], and bone is also a good candidate for SEM [12,16-19]. The low water content alone means that preparative distortion is low [14,20]. The high mineral content means that there is sufficient of it to hold together after removal of the organic matrix to make a specimen which contains no structural water, and which will, therefore, not shrink when dried; such "anorganic" or "deproteinised" specimens are attractively easy to prepare, and reveal a wealth of easily interpretable information concerning the past history and the functional status of bone surfaces using the conventional, standard approach of secondary electron (SE) imaging in the SEM [12,62,63]. Whereas most vertebrate tissues have a nearly uniform mass distribution (when interrogated at a pixel size scale of the order of 0.1 μm), bone is exceptional in showing both a much higher density and local variation in density which convey valuable information about the past history of growth and remodelling in the bone tissue [2,6-11,32].

This class of information - concerning density - can be obtained most easily by using the fast, back scattered electrons (BSE) in the SEM [14, 15, 22, 28, 29,63,65]: it is, however, also carried by the SE, since an important portion of these arise through the interaction of BSE with the surface layers of the specimen, and there are more, returning BSE from denser regions of the samples. Nevertheless at present we consider BSE as the signal to use for analysing density differences. To be able to do so, we need to be able to exclude the element of contrast in BSE images which is due to the surface roughness of the specimen. To do this, we embed specimens in a plastic and cut and polish the surface of the hardened block. The plastic that we have chosen is polymethylmethacrylate (PMMA), because its monomer has a low viscosity and therefore penetrates well into this difficult-to-embed tissue. As is known from the early days of TEM, however, PMMA is unstable under electron bombardment. We, therefore, add a ring compound

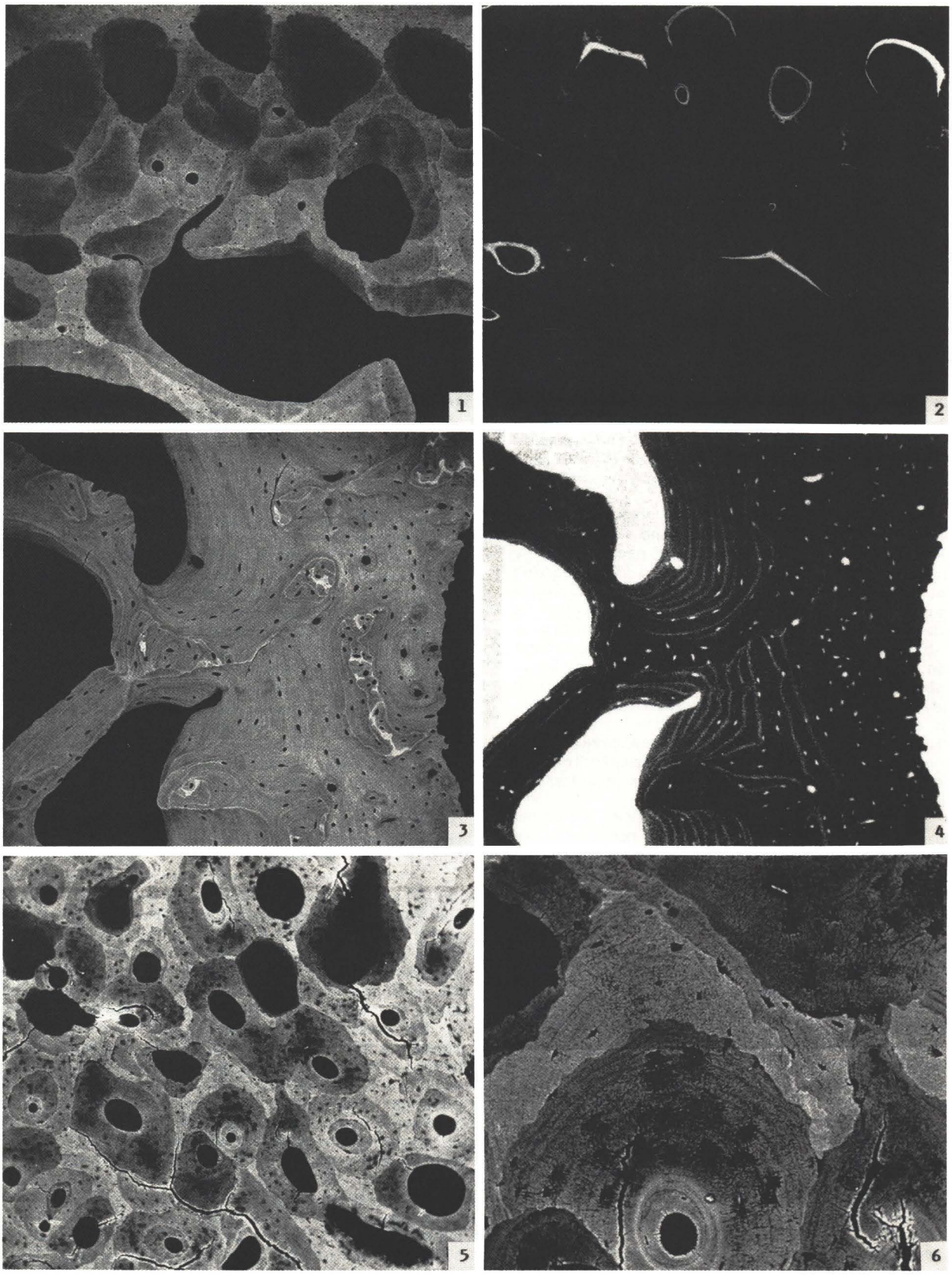
1
2
3
4
5
6

Figures 1 and 2. BSE and CL images of carbon coated, polished block face of normal 9 yr human femur TS: showing range of densities of bone in BSE (fig. 1) and **detection of osteoid by CL** stain in fig 2. Fieldwidths = 1710µm.
Figures 3 and 4. TS 4 month rat tibia given weekly tetracycline injections. BSE (fig. 3) shows marrow space as black, calcified cartilage remnants as white, osteocyte lacunae as smaller and blood vessel canals as larger dark feature in bone. **CL (fig. 4) shows tetracycline lines** and marrow space as white due to inclusion of PPO in embedding PMMA. Fieldwidths = 750µm.
Figures 5 and 6. BSE: TS compact bone in case of vitamin D resistant rickets **(courtesy of Prof. R.** Steendijk). Note high incidence of perilacunar mineralisation deficiencies. Fieldwidths = 1810µm in Fig. 5 and 480µm in Fig 6.

monomer, styrene, to our PMMA mix to produce a stable block material[1,4,25,28,63,65].

PMMA and Bio plastic™ are used widely as embedding agents for LM studies of bone biopsy samples taken in the routine clinical investigation of metabolic-bone diseases, so that large numbers of blocks are available for retrospective study[10,11,32-36,39,45-54,66,74]. It is also possible to study these blocks by BSE-SEM, but greater caution has to be taken not to leave the beam stationary for too long on any one patch of the surface.

A third attractive feature of SEM as an approach to studying bone is that it is a **scanning** technique. Thus information is obtained point by point (the basic procedure in stereology) and it is in a form (a DC voltage output) which is computer compatible. It is therefore a very simple matter to digitise the output signal and to digitise the scan pattern and signal - and then one has an "image analysis system". This is significant if the signal level has a real physical meaning. As just noted, the BSE signal from a flat surface satisfies this criterion[14, 15, 22,42,65]. A flat surface can only be generated on a specimen in which the "holes" are filled in - hence the need for embedding[14].

Image Analysis

An important requirement in the analysis of the SEM image of a block surface of bone is to be able to recognise, preferably by automatic means, non-mineralised bone matrix (osteoid) from other tissue components (it would also be desirable to be able to "read" the cells in the block surface - see later). The density of the usual organic embedding resins is very close to that of structural biopolymers, so that neither SE nor BSE signals can permit this to be done by machine. We have found a set of solutions to this problem based upon the use of another one of the signals resulting from electron bombardment - namely the emission of light (cathodoluminescence, CL). By including a scintillating agent in the embedding medium we can make all parts of the bone block emit CL, except the dense bone and osteoid. Alternatively, we may stain the osteoid with an appropriate CL stain (e.g. brilliant sulphaflavine), so that it emits more CL than any other phase (figs 1 and 2)[25-28]. If we can quantify the CL signal synchronously (or subsequently) with the BSE signal, then, we can measure osteoid as distinct from bone, bone as distinct from anything else, and subdivide the bone into mineralisation - density fractions. Marrow space, including all the cells, is the proportion left over. The CL signal can also be used to read tetracycline lines in bone in the SEM (figs 3 and 4)[27].

We have been evolving improvements to SEM techniques with this object in mind - to develop a routine diagnostic and analytical tool for bone pathology. We have presently advanced to the point where we would feel confident in stating that our technology clearly excels any other that has yet been proposed for quantitating bone and osteoid volumes[22,28,63]; no other routine procedure has been established for the fractionation of bone density. The microradiographic, thick ground section approach does not seem to have led to any published results[61]. We first justify this level of assurance, and then point to deficiencies and limitations of such approaches as we have so far considered.

Light Microscopy (LM) vs SEM

LM stereology of undecalcified sections (5 to 20 µm thick) of PMMA embedded bone ("bone histomorphometry") has disadvantages which we have overcome by SEM based techniques. (1) The section does not approach the infinite thinness required of the fundamental stereological principle - which in the first instance assumed the cut face of a block! (2) Microtomed sections are deformed and distorted to a significant degree. (3) The staining methods used to distinguish bone from osteoid (severely hampered by restraint (1)) contain no fundamental guarantee that they are correct[53].

However, LM sections enable one to recognise types and grades of cells on the bone surface, as well as bone marrow changes (such as invasion by tumor metastases or the fibrosis found in hyperparathyroidism[54,74]). The disability of our SEM methods in this respect has led us to explore other methods of block surface microscopy in order that we might overcome these limitations. The objection that we could not "read" tetracycline labels was removed by the discovery that we could image these with CL[27].

A variety of stains - mainly fluorescent - can be used to produce good quality images of bone cells in the superficial layers of entire PMMA or glycol methacrylate blocks[5]. The LM imaging of fluorescent, and pseudo-fluorescent or reflective stains, can be significantly improved by reducing the thickness of the layer from which the returning signal derives by some means of optical sectioning. We have used the tandem scanning reflected light microscope (TSRLM) for this purpose[24,60].

At present, it would be more efficient to employ the classical LM sectioning procedures and staining schedules in laboratories which are suitably equipped and skilled. This enables osteoblasts to be seen as active, or quiescent, and osteoclasts to be seen in Howship's lacunae or "off the surface", for example. However, block surface fluorescence microscopy with a standard epifluorescence LM is a practical alternative: the same information can be acquired and without the need for microtomy[5].

Regarding the TSRLM, this instrument is presently a rarity. We have found two major advantages for it: (a) that it can be used to study the distribution of tetracycline labels in three dimensions (figure 14). Tetracycline is administered usually orally at known times: these antibiotics bind to the mineralising front in bone. By timing the intervals between "labels" and measuring the physical distance between them in the bone tissue in the biopsy it is possible to quantitate both the local rate of bone formation (mineralisation) and the proportional extent of bone formative surfaces[39,74]. With the TSRLM, we can both see where it is permissible to make a direct measurement of the gap between adjacent labels, and survey a much greater volume of tissue. We can realistically analyse a 100 μm layer in the block surface: this is a great improvement over the patchy analysis of one or two 20 μm thick sections. In addition, we have shown that it is possible to exploit the brilliant sulphaflavine (BS) stained blocks in the TSRLM. Here, the fluorescent staining is the converse of the degree of mineralisation of the bone, with osteoid intensely fluorescent. It would therefore be possible to use the fluorescent mode in a TSRLM to quantitate bone and osteoid, at several optical-section levels, and at a few mineralisation density levels.

Materials and Methods

The basic philosophy of our approach to using SEM in bone pathology is intimately wrapped up with the methodology, just reviewed in the introduction. Here we take the pragmatic, technical approach and describe the outlines of procedures which we have used extensively.

Materials

Bone samples were obtained by trephine biopsy of the iliac crest[36,37,69]; from long bones at operation for the correction of a deformity[64,69]; and from a variety of sites at post mortem[38,62,63,65]. All of our biopsy material was taken for another purpose, usually routine bone histomophometry. The variety of disease conditions examined is indicated in the observations. Fixation was usually in neutral formol saline for a few days. Where we have obtained the tissue directly, we have used 70% ethanol as fixative and preservative to avoid any possibility of demineralisation due to the degradation of formaldehyde to formic acid. A further reason for this choice was to prevent aldehyde fixation stopping the action of trypsin in cleaning cells from osteoid surfaces. (Carnoy's fixative has been used for LM bone histomorphometry[34], but should be avoided because of its acetic acid content).

Whole Bone Preparations

Bone marrow and cells adherent to bone surfaces were cleaned away with a water jet. Trypsin solutions were sometimes used to aid this process. Such preparations were air dried from a volatile solvent such as $C_2Cl_3F_3$, ethanol or acetone and gold sputter coated. The purpose of examining such preparations would be to characterise: (a) the 3D morphology at low magnifications: (b) the nature of the bone surface, particularly the pattern of the collagen fibre weave in the matrix, and the details of resorptive surfaces.

Anorganic preparations

Much more useful, and much more economic to produce are anorganic specimens: these give immediate information about the character of the bone surface - whether resorbing, resorbed recently, resorbed some time ago, whether resting (matrix mineralised to the limits of the collagen phase) or prolonged resting (matrix mineralised into ground substance beyond the peripheral collagen at the surface of the osteoid): or whether "mineralising". In the last case, however, we have shown that finer criteria are required than the previously accepted view that all partly-mineralised-collagen covered surfaces are mineralising. Particularly in pathologies, many of these are arrested mineralising fronts. We have been able to recognise some of these as having a different character than those which we can prove to be active from dynamic tetracyline labelling data.

Although, not strictly "anorganic" because only the superficial osteoid is dissolved, hydrogen peroxide treated bone samples are the most robust and this would be the technique to be recommended in routine tissue handling delegated to less skilled technical staff. It is better to defat the above using chloroform-methanol before beginning.

Really anorganic samples are fragile, but may be safely air-dried from water: the absence of water bound to organic matrix removes the shrinkage inducing factor. We have used:
(a) sodium hypochlorite as the concentrated reagent (household bleach, Chlorox in American English) diluted with an equal volume of water: we designate this as 5-7% NaOCl because the stock is given as 14% when fresh.
(b) Sodium peroxide, used as a crudely estimated 2% solution in water at 50°C[23].
(c) we eschew the use of 1,2 ethane diamine[16,17] and hydrazine because of their toxicity: they are dangerous to use.

PMMA embedding

We defat and dehydrate the fixed tissue blocks by refluxing with chloroform-methanol in a Soxhlet apparatus. We flash distil* the methyl methacrylate monomer under vacuum to remove the

added stabilising agent, hydroquinone. (* A flask of monomer is frozen using liquid nitrogen: the air is then evacuated from the flask and the U-tube connecting it to another flask: the latter is now surrounded by liquid nitrogen. The monomer now condenses in the cooler flask as the former warms up). Polymerisation is induced by an activator and warming to 32°C after several changes of the monomer mixture with 5% styrene monomer[14,63]. The above procedure is rigorous and time consuming, but avoids the dangers of the process used in normal clinical pathological laboratories which induces bubbling in the methacrylate caused by too rapid polymerisation, leading to a temperature rise; with the added tendency to bubbling (figure 13) caused by traces of residual water from solution exchange dehydration schedules. Notwithstanding, we have made many successful studies in routinely prepared blocks (e.g. figs. 15 and 16), and these should not be shunned if the embedding looks good when inspected under a stereo microscope.

PMMA block faces were examined either (a) as left cut after the last section had been taken by the pathological laboratory (fig. 18); or (b) after polishing on graded abrasives, finishing with water dispersed diamond on a rotary lap (figs.1-6,11,12,17 and 24); or (c) diamond micromilling[14](figure 13). The PMMA block faces were coated with carbon to render them electrically conductive and to keep the density of the conductive coat as low as possible in order not to interfere with the BSE signal.

Removal of methacrylate

A further advantage is gained through using carbon coatings:- that they may be removed together with a controllable thickness of the PMMA from the block surface zone using oxygen plasma ashing. Acetone, xylene, or chloroform may be used to dissolve PMMA to leave the bone exposed for conventional SE-SEM imaging[35].

SEM methods

SE Imaging: We use a conventional Everhart-Thornley biassed scintillator detector. Since we are dealing with 3-D topography, we record stereo-pair images with a defined tilt angle difference so that they may also be used for stereophotogrammetric analysis[21,41]. To minimise penetration and charging artifacts we normally work at 10kV accelerating voltage and about 10^{-11} Amps probe current.

BSE Imaging: We use a solid state BSE detector (KE Developments, The Mount, Toft, Cambs, U.K.). This has four sectors. We normally add the signal from all sectors to give a ring configuration. Thus the detector views a normal incidence specimen at mean normal incidence. We work at 20kV beam voltage and about 10^{-9} Amps beam current.

Cathodoluminescence: We have described the design of our simple CL collectors elsewhere[26]: we work under operating conditions identical to those used for BSE imaging[25].

Image Analysis Systems: Originally, we worked with a Quantimet 720 image analysis system which could be used either with a TV camera input from a light microscope[36] or to control the scan generator and to measure the signal level at each pixel in an SEM image[15,28] (figure 18). Image analysis proved to be essentially useless until we could select the fast electron signal to measure bone reliably, first achieved using converted backscattered electron (CBSE) imaging[14,15].

The Quantimet system was not sufficiently versatile for our immediate needs, because only 3 threshold levels, thus 4 density fractions, could be selected simultaneously. The digital image analysis was, therefore, too restricted and limited by our ability to set the thresholds the same on different occasions. However, the most important difficulty turned out to be the instability of the entire SEM system.

We therefore designed and constructed a home made image analysis system based on a Sharp MZ80K microcomputer, which acted as scan generator via a digital to analog and image analyser via an analog to digital[42,63,65]. Using this system we have chosen to divide the bone density data into 8 thresholded bins, 1 to represent non-bone and 2 to 8 to contain the histogram of the proportion of bone conforming to particular density images[65].

Normative data

A large difficulty in the use of SEM in bone pathology is that we have lacked information about the range of appearances in qualitative SE imaging, and any quantitative SE or BSE data in normal subjects as a function of age, sex and skeletal site, never mind any variations due to abnormal function. (Good developmental data only existed for conventional histology and microradiography[39,44]). We therefore undertook a study of this nature, which has so far progressed to the detailed examination of bone surface conditions and mineral density distributions as a function of age in human sixth ribs[63,65]. This detailed study has confirmed our prior interpretations based upon a far more sporadic human data base and utilising information obtained from the study of bone samples from a variety of mammalian species[12,16,17,19,20]. There is no doubt, however, that the study of normal tissue must urgently be extended, first to cover a large number of iliac crest biopsies from "normal" subjects, because this is the site adopted in most published studies; and second to examine the possibility that image analysis of the "texture" of the surface of patches of bone samples in a statistically satisfactory fashion, could lead to an extremely simple means for the diagnostic indexing of bone surface activity states. Thus it would certainly be possible to recognise forming, resting and resorbing mature lamellar bone surfaces on the basis of counting the number of "features" defined by a single grey level threshold applied to SE images of simply-prepared anorganic bone samples. Present techniques for indexing the ratios of types of

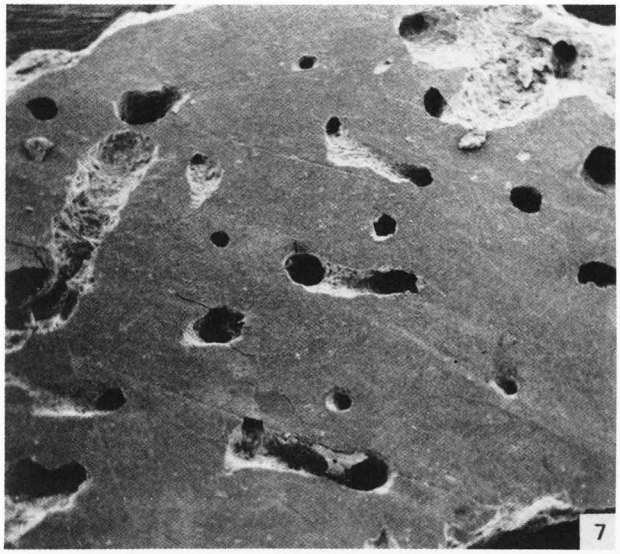
7


8

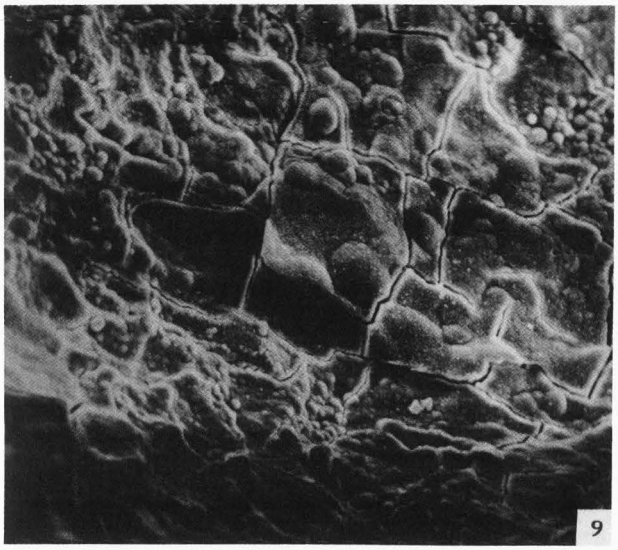
9


10

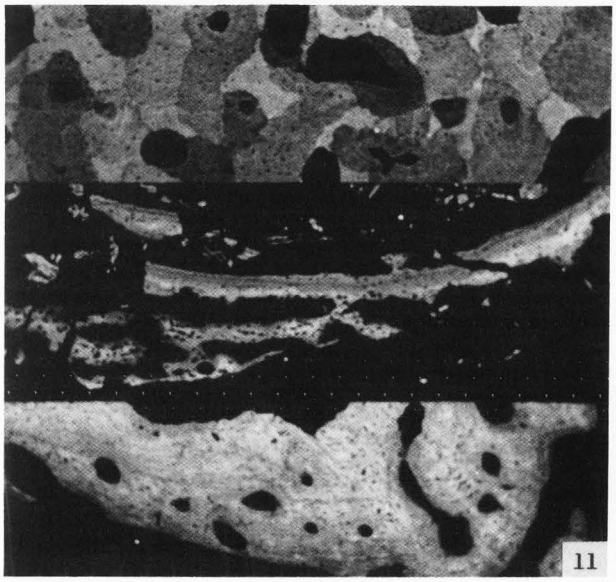
11

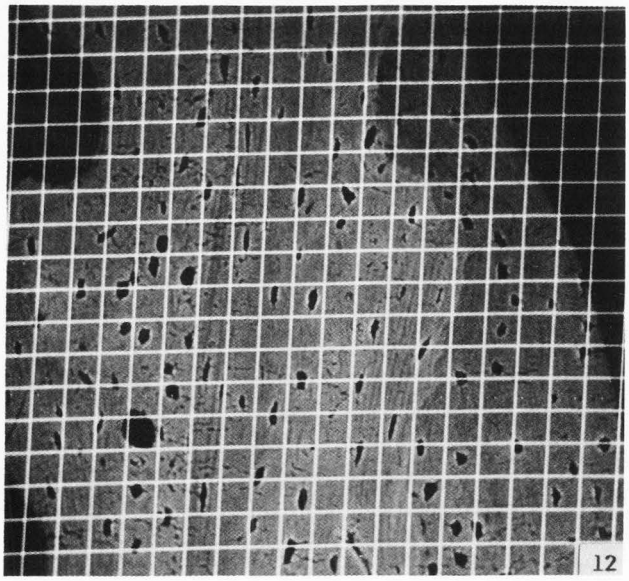
12

Figures 7, 8 & 9. Osteopetrosis. SE images of tooth supporting bone removed whilst extracting premolar. **Fig. 7** shows the small marrow space volume. **Fig. 8** shows a resorptive surface at a canal lining. **Fig. 9** shows the lining of a canal with mineralisation in a non-collagenous matrix: this has cracked and charged due to inadequate conductive coating - picture taken before CBSE or BSE images were available. Fieldwidths: Fig. 7= 2050µm. Fig.8= 98µm. Fig. 9=84µm.
Figure 10. Bone removed from mandible in case of **fibrous dysplasia** (specimen courtesy J. Blenkinsop). Surface of matrix: note random fiber orientation typical of foetal bone: in this condition, however, the number of lacunae is less than in normal lamellar bone. Fieldwidth = 17µm.
Figure 11. BSE: strips 1 and 2 show areas of bone from 2 cases of **osteogenesis imperfecta** (OI2 and OI1, respectively): the third strip shows normal 9 year old bone as an age matched control. In order to demonstrate real density differences and to avoid difficulties due to instrumental drift, differences in photographic exposure and processing etc., were recorded on one photo negative on one occasion, moving the three specimens under the beam in quick succession. Field lengths along strips = 1950µm.
Figure 12. Osteogenesis imperfecta: case OI2, showing scan generator generated stereological grid method[17] for the measurement of the volume fraction occupied by osteocyte lacunae; which proven, at 4%, to be twice the value in age matched control bone. Fieldwidth = 450µm.

←

bone surface condition may be regarded as adequate for present needs only because the pathologist is confined to identifying gross excursions from the normal range. We do the same in the presentation of examples of findings from selected bone pathologies in the following.

Table 1. Percent of mineralised bone falling within equal width density ranges covering the extremes of values found for "bone" through calcified cartilage[63,65]. Human sixth rib autopsies.

	Bin						
	1	2	3	4	5	6	7
4 Neonates	6	17	33	29	11	1	0
10y+ 13y	3	9	23	41	20	1	0
4 adults	0	1	6	26	52	11	0

SEM results

Familial hypophosphatemia - Vitamin D resistant rickets (VDRR). Studies with R. Steendijk[69].

The hallmarks of this disease from the viewpoint of SEM imaging are the circumlacunar mineralisation defect, and the common occurrence of a complete failure of mineralisation at some cement lines[11,32,69]. Examination of formative surfaces in anorganic preparations shows half-formed osteocyte lacunae with the collagen in their back walls incompletely mineralised. In normal lamellar bone, the collagen bundles and fibres are completely mineralised at the level where mineralisation in surrounding matrix - made by osteoblasts other than the encapsulated osteocyte - clearly demarcates the lacuna[11,16,19,62]. The imperfection of mineralisation of the collagen seen on the centrifugal side of lacunae is exaggerated on their centripetal aspects[32,69]. Thus in a cut bone surface made anorganic there are obviously more defects towards the centre of each osteon: in BSE imaging of PMMA blocks, the unequal distribution of this circumlacunar "beard" of incomplete mineralisation is clearly seen (figs. 5 and 6).

The presence of non-mineralised layers at any level during the closure of osteons is also interesting[69]. Dissolving non-mineralised matrix takes away complete layers of bone, showing that the mineralisation process stopped, and after an interval started again at a more superficial level. Both these phenomena indicate that, at least in this disease, osteoid does not mineralise at all if it does not mineralise on schedule.

Osteopetrosis

The name osteopetrosis implies that there is more bone tissue per unit volume of bone than found within the normal range. Examination of specimens of alveolar bone removed during exodontia from an adult patient with this condition confirmed the high volume fraction of bone (Fig.7). However, it was also found that many of the free bone surfaces were covered with apparently normal resorption lacunae (Fig. 8). At the time that these observations were made (1978 - unpublished), this was found to be surprising. It indicated that competent osteoclasts were present, so that contrary to some prevailing opinions, the failure to remove bone in remodelling was only relative.

Another interesting finding was that many of the lining surfaces were covered with a relatively thick layer of calcified material with a smooth, rounded, flattened-knobbly surface (Fig. 9). This material did not contain collagen, so represented mineralisation in an abnormal "ground substance" matrix. Some canals were more or less completely blocked with this material.[3]

Fibrogenesis imperfecta ossium

Study with R. Smith (in preparation).

Fibrogenesis imperfecta ossium is a rare connective tissue disorder in which patients suffer progressive bone pain and fracturing, leading to immobility. It is characterised histologically by the presence of thick osteoid seams which are non birefringent when seen in polarised light. The fibrous component of these seams is a tangled mat of fine fibrils which replaces the normal lamellar organisation of much thicker collagen fibrils.

Parts of two iliac crest biopsies taken from the same 51 year old male Caucasian were studied. These were taken 12 months apart and prior to each one the patient followed a tetracycline

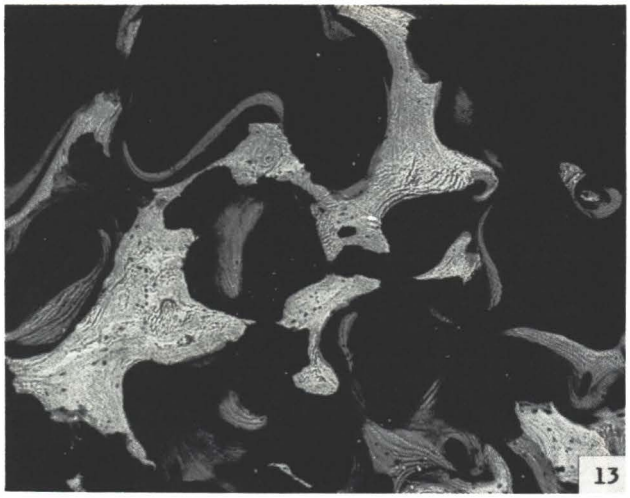

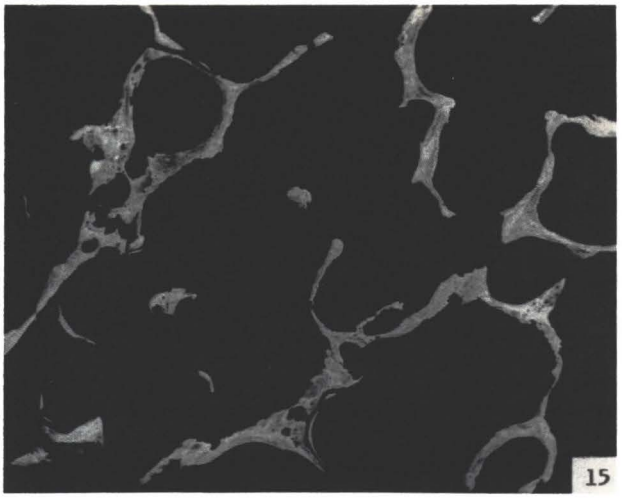

Captions on facing page.

Figure 14a. Focus 10μm below block face.

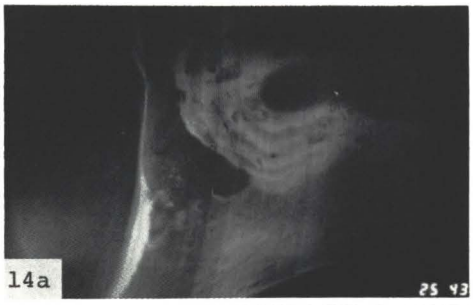

Figure 14b. Focus 35μm below block face.

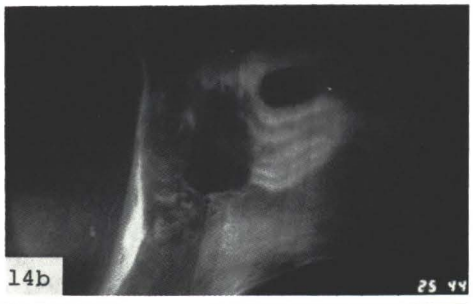

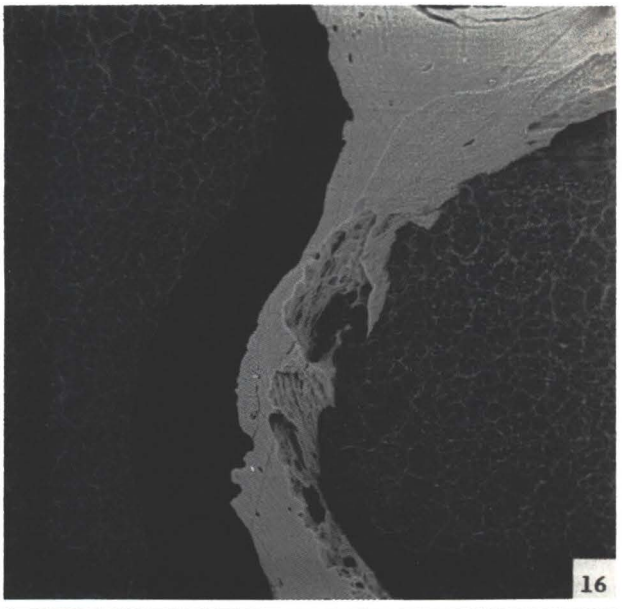

Figure 14c. Focus 60μm below block face.

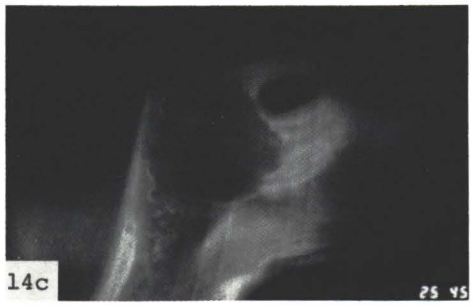

Figure 14d. Focus 85μm below block face.

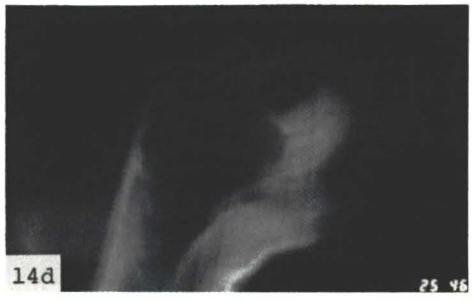

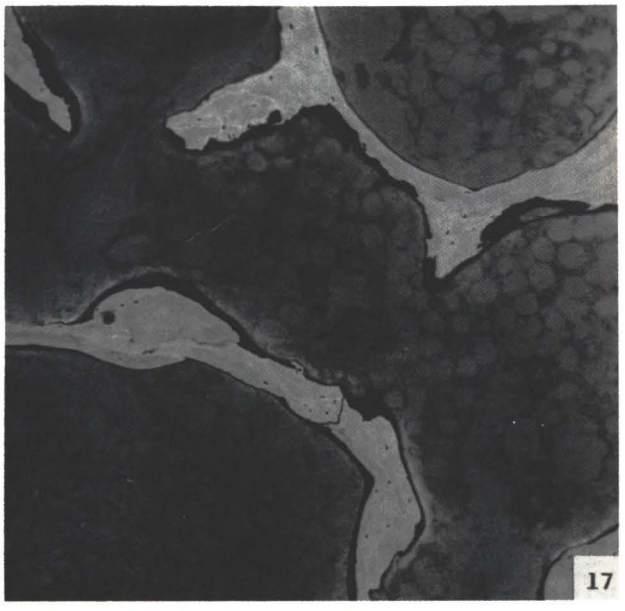

Figure 13. Adult rickets. Case of nutritional **osteomalacia** (specimen courtesy S.T.S. Teotia). Pattern of distribution of mineralised bone shows many areas which must be osteoid; these can be recognised in topographic images due to the more imperfect finish, revealing lamellae, compared with the PMMA embedded marrow. Micromilled surface finish. BSE: PMMA block as received was poorly embedded and bubbling can be seen. Fieldwidth = 1980µm.

Figure 14. Iliac crest biopsy of case of severe **osteomalacia in renal failure.** PMMA block face imaged using 20/0.8 glycerine immersion objective **in the TSRLM.** Through focus sequence at 25µm intervals. Violet excitation. Yellow pass filter. 5 Fluorescent lines due to weekly tetracycline administration. Bone formed within the 5 week period before the biopsy was taken has already been resorbed: note resorption cavity seen at deeper focus levels. Fieldwidths = 400µm.

Figs. 15 & 16. Osteomalacia in renal failure. Iliac crest biopsy.

Fig. 15. Overview of block face showing paucity of mineralised bone, sites of dissecting resorption, and arrested mineralising fronts. Fieldwidth = 4330µm.

Fig. 16. Part of same block after plasma ashing to remove PMMA (and osteoid. All surfaces are either resorbed or show incomplete matrix mineralisation. Fieldwidth = 874µm.

Figure 17. Aluminium osteopathy, iliac crest biopsy: osteomalacia of renal dialysis complicated by Al "poisoning" of mineralising fronts (case provided by B. Boyce). Combined BSE and CL image. Mineralised bone appears white because of its natural mineral content: marrow space appears white because of PPO scintillator incorporated in embedding PMMA. Osteoid appears black: the signal difference is sufficient to permit automatic on line analysis of osteoid volume etc. Fieldwidth = 1380µm.

←

---

double labelling regime. Light microscopic histology revealed a paucity of bone, especially in the second biopsy. Many surfaces were lined by thick osteoid seams and the use of polarised light confirmed that these were non-birefringent. Fluorescent microscopy using the TSRLM demonstrated tetracycline fluorescence at many of the surfaces line with osteoid. However, separate labels could never be resolved and it was concluded that mineralisation was either proceeding very slowly, or was occurring within a considerable thickness of tissue at any one time. Secondary electron imaging in the SEM of surfaces cleaned to reveal matrix and mineral fronts showed that the pattern of mineralisation was abnormal. This was confirmed by BSE imaging in the SEM of polished, cut surfaces of plastic embedded material. Combined BSE and CL investigation demonstrated that the non-birefringent bone matrix sometimes attained a substantially greater mineral density than normal.

Fibrous dysplasia[70]

Examination of several bone fragments from one patient with polyostotic fibrous dysplasia showed that large areas of the matrix surface showed the random fibre orientation typical of foetal (woven) bone, but had the opposite character of a reduced number of lacunae compared with normal adult lamellar bone (Fig. 10).

Osteogenesis Imperfecta[49,59,64,73]

We have examined material from 3 biopsies: (1) tibia, 70% ethanol fixation, 7 year female, (2) tibia, frozen, 70% ethanol, 8.5 year female (3) iliac crest, formalin, received demineralised: For polarised light microscopy (PLM) ground sections were prepared from the plastic embedded block faces of 1, and 2.

The OI samples showed very thin cortices, composed mostly of lamellar bone, with few osteons and surrounding foetal or woven bone in case 1. SE images of 1, 2 and 3 showed normal matrix surface features, with the branching bundle pattern of normal lamellar bone, but the mineral front preparations (of 1 and 2) revealed that all surfaces were either mineralising (forming), or resorbing or resorbed: no resting, fully mineralised surfaces were found. Against this, it should be remembered that the proportion of resting surfaces is greatly reduced in the bone of growing children[62,63]. Cut - or fractured-open osteocyte lacunar walls showed intact collagen. The finding of incompletely mineralised collagen bundles in lacunar walls in anorganic preparations cannot be taken as evidence in favour of "osteocytic osteolysis"[7,10,13,33,53,54,76,77] since similar incompletely mineralised collagen could be demonstrated in the back walls of half-formed lacunae at the mineralising front, unlike the control situation. BSE imaging revealed density differences in OI: in case 1, the most densely mineralised bone was denser than any phase in a 9-year control, but equivalent to the densest phase in adult bone. In case 2, most of the bone belonged to very dense phase (Fig. 11). Use of an SEM-generated stereological grid counting technique[18] for the fractional volume of bone occupied by osteocyte lacunae showed 8% in case 1 (distorted upwards by foetal bone values), 4% in case 2 (Fig 12), and 2% in 9 - year control. PLM showed OI lamellae to be roughly half the thickness of normals.

OI osteoblasts thus produce much less matrix than normal, remaining themselves, as osteocytes, towards the top end of the normal size distribution. An unusual degree of resorption further reduces the total bone volume, which further has a limited degree of interconnection between adjacent layers.[64]. The tendency to fracture is again increased by the higher degree of mineralisation of the inadequate quantity of bone.

Our results do not concur with those of an earlier report[73] of a parallel fibred matrix with few lacunae in 3 cases of OI. We believe that this matrix may be a phase other than bone, since we found a rubbery unmineralised tissue incorporated in the bone in one of our specimens.

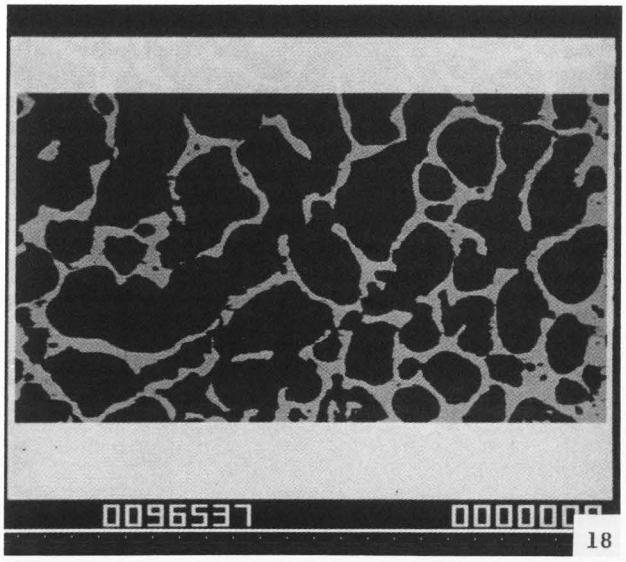

18

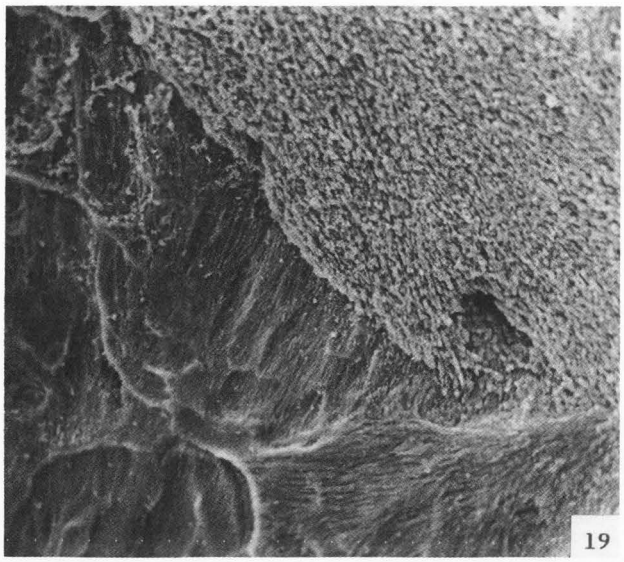

19

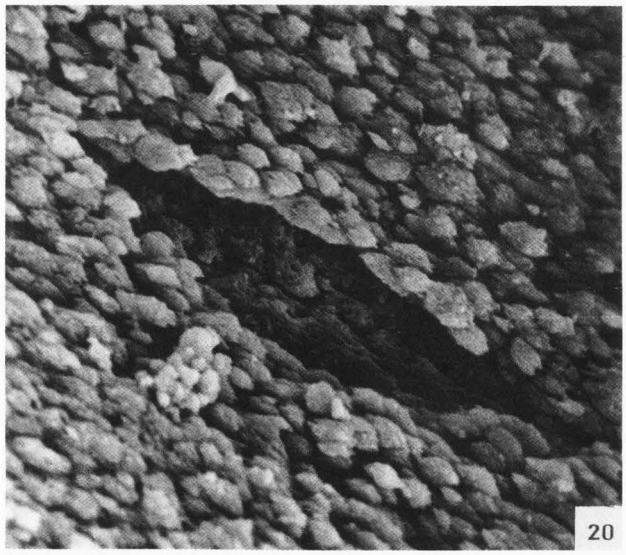

20

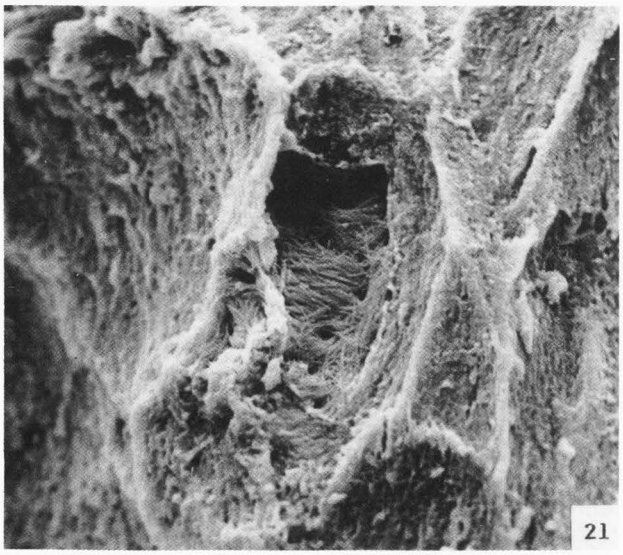

21

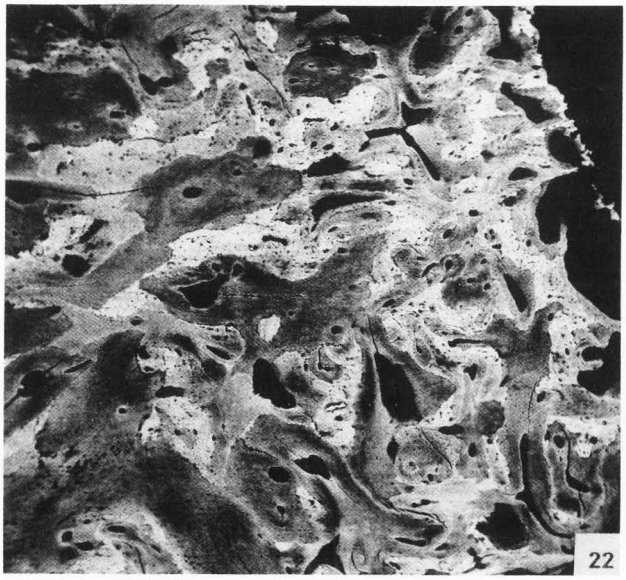

22

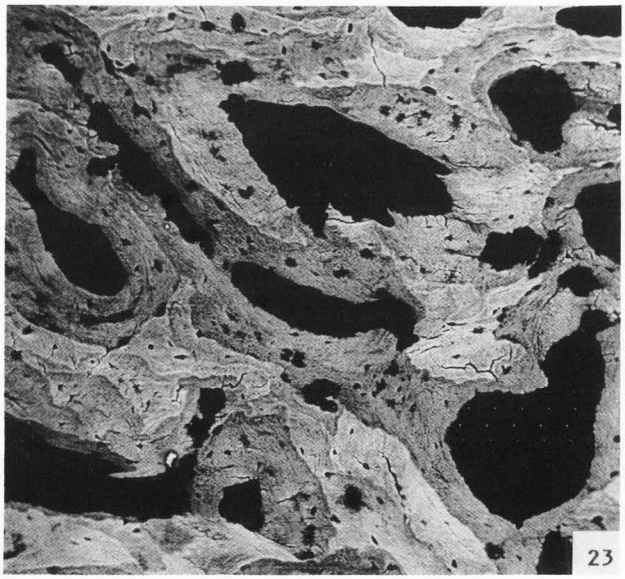

23

Figure 18. Rapid measurement of bone volume etc. Iliac crest biopsy, normal case (courtesy of I. Bab); BSE, Quantimet 720 detected area image: Area was 22.9% of active frame. By placing the block at a large working distance, as done here, it is possible to obtain a very low magnification (here about 8X) so as to encompass the entire trabecular bone region in one frame. By using the variable frame of the Quantimet, we could exclude the cortical compact bone and areas outside the biopsy. This leads to a very rapid method to measure the entire trabecular bone volume fraction. Fieldwith = 9600µm.

Figures 19, 20 and 21. Primary hyperparathyroidism, autopsy sample from vertebral body. SE images of anorganic surfaces of trabecular bone, which were all either resorbing or resorbed or showed incomplete mineralisation indicative of active formation.
Fig. 19 is a low power view showing that half of this surface was resorbed and half was actively forming. Fieldwidth = 161µm.
Fig. 20: half-formed lacuna in mineralising front showing incomplete mineralisation in lacunar wall. Fieldwidth = 34µm.
Fig. 21 shows that resorption into older bone lacunae reveals intact collagen in lacunar walls, contradicting possibility of osteocytic osteolysis. Fieldwidth = 35µm.
Figures 22 and 23. Biopsies from two cases of **endemic fluorosis** (courtesy of J.M. Faccini and S.P.S. Teotia; blocks 2 and 11 respectively of their 1974[37] study). BSE images of micromilled PMMA block faces showing the density of the bone, the atypical remodelling, the numerous large lacunae, some of which are surrounded by circumlacunar mineralisation defects. Fieldwidths, Fig. 22 = 4950µm. Fig. 23 = 990µm.

←

Rickets

Rickets is a condition which results from a lack of dietary vitamin D and/or of sunlight, which may be combined with an inadequate Ca intake, during the growth period. We have not studied any material of human origin, but have studied avian rickets[29]. Of importance here is the observation that the mineralisation of bone deposited on rachitic calcified cartilage may start away from the cartilage, leaving a layer of unmineralised osteoid. According to our experience, this seems to be generally the case in all forms of rickets as studied by SEM, including VDRR, and renal bone diease.

Osteomalacia, Renal Bone Disease and Secondary Hyperparathyroidism.

Osteomalacia is a common condition which is caused by intestinal malabsorption or is often the complication of renal disease: Adult rickets due to dietary vitamin D insufficiency is common in patients from the Indian subcontinent (figure 13).

Renal bone disease has characteristics related to abnormal vitamin D metabolism and the secondary hyperparathyroidism accompanying the kidney malfunction. Elevated parathyroid hormone (PTH) levels separately increase both bone formation and resorption[71]. Histology thus shows both a tendency towards the presence of large amounts of more, rapidly assembled, immature forms of bone containing enlarged lacunae with imperfectly mineralised walls; many areas of recent resorption, and defective mineralisation attributable to the vitamin D problem[4,6,30,34,45-48,50,53,54,66,67].

A case of severe renal (dialysis) bone disease serves to illustrate the usefulness of the TSRLM in studying tetracyline label distributions to map turnover. Figure 14 shows images recorded at 25µm intervals below the surface of a routine PMMA block, untouched since the last section was cut from the block face. The patient was given 5 courses of tetracycline at one week intervals. The most superficial level shows all the labels. At deeper levels some of this recently formed bone has already been resorbed: this is a high bone turnover disease!

Examination of PMMA block faces from cases of osteomalacia reveals a high incidence of failure to mineralise. Extensive patches of osteoid cover reversal lines marking the progress of prior resorptive episodes (fig.15).

The high level of remodelling resorption in renal bone disease frequently involves a process known as dissecting resorption (figs. 15 and 16). Whereas it is clearly the case that osteoid can be resorbed by activated osteoclasts, there is also a clear preference for mineralised bone matrix. Since much of the bone is covered by osteoid, calcified bone can only be found by digging underneath this layer.

Aluminium associated renal dialysis bone disease. Study with B. Boyce

Al in the water used to make the dialysis fluid for patients with severe renal insufficiency is now known to exacerbate the resulting bone disease: it "poisons" the mineral clusters which initiate the mineralisation process in newly formed matrix[11].

Figure 17 shows an example of the CL + BSE signal processing approach to distinguish osteoid, and illustrates the high osteoid fractional volume in this condition.

In all the disease processes where mineralisation fails more or less completely and osteoid therefore accumulates, there is bound to be a gross discrepancy between the appearance of the matrix surface preparations for SE imaging and those of the mineral front. These remarks, therefore, apply to all the examples of "histological osteomalacia" considered in this review, including some areas of VDRR, OI, and osteomalacia. Making the sample anorganic - in the case of PMMA blocks, by plasma ashing[14] - removes both PMMA and osteoid. Because of the high bone turnover, there are very extensive reversal surfaces. In the mineral front preparation, then, we see an increased fraction of resorbed surfaces: we are unable to visualise the fact that they had been covered

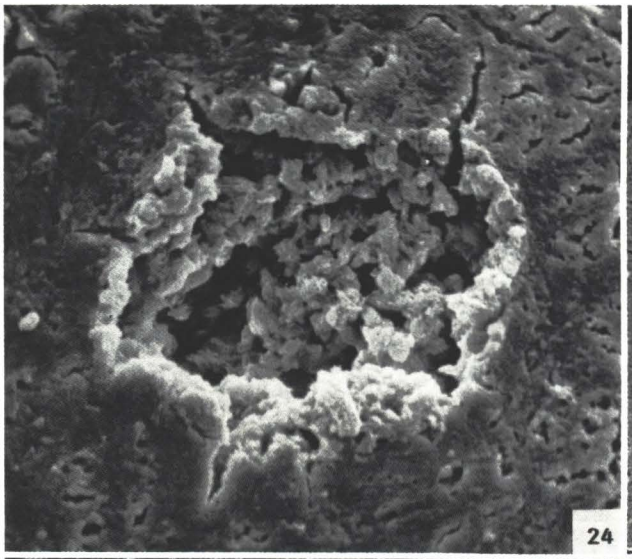
24

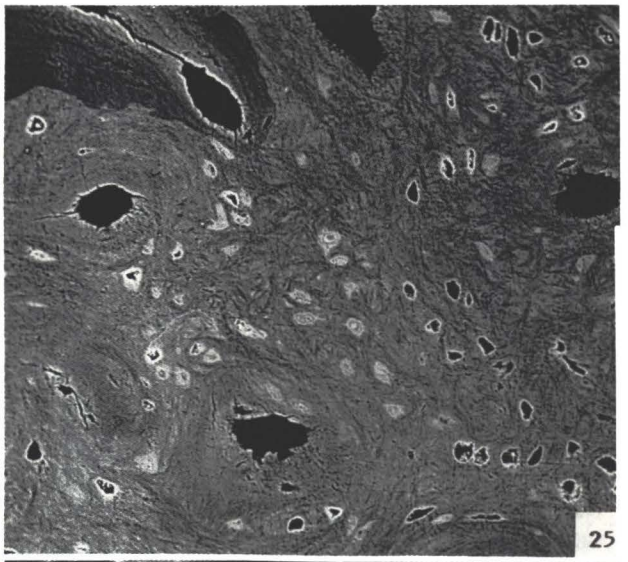
25

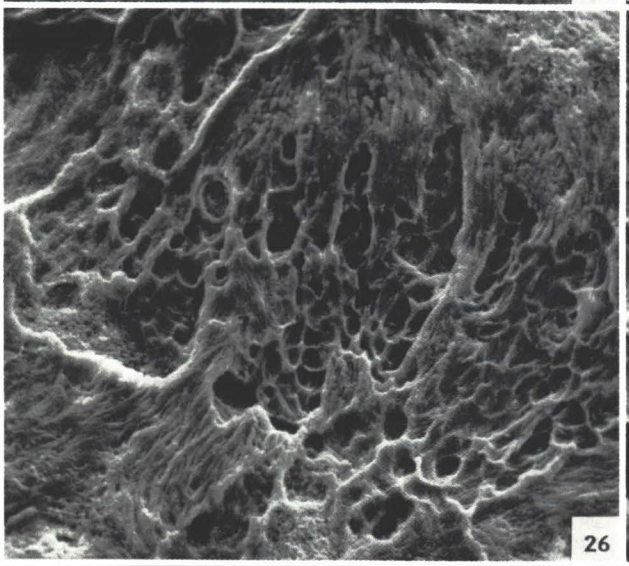
26

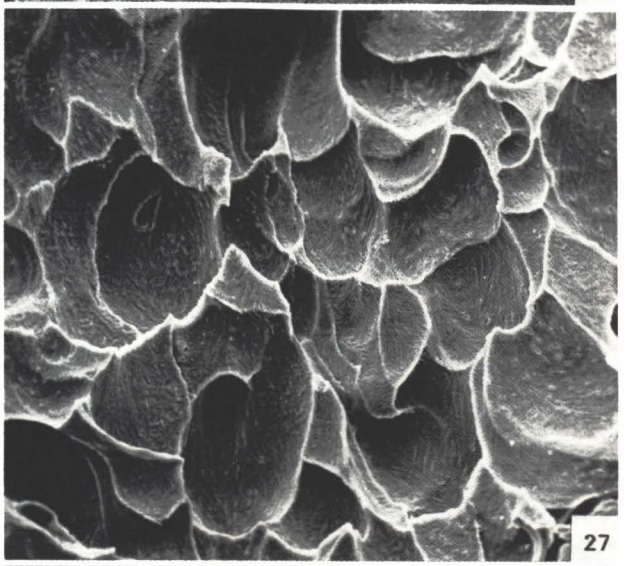
27

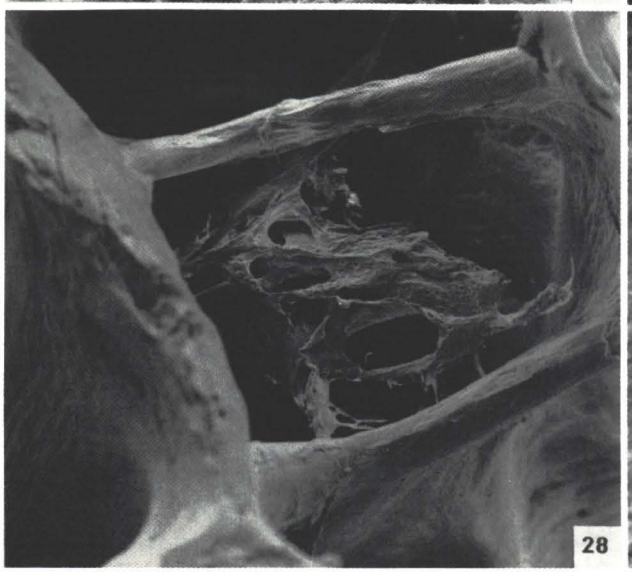
28

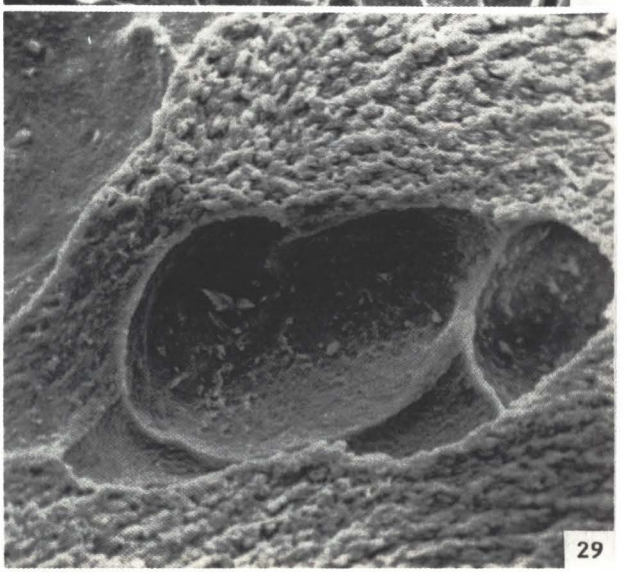
29

Figure 24. Paget's disease (autopsy courtesy M. Nimni). Anorganic cut surface showing incomplete mineralisation in the matrix surrounding an osteocyte lacuna. Fieldwidth = 15µm.

Figure 25. Incus. BSE showing occlusion of osteocyte lacunae with dense mineralised phase which includes the remnants of the osteocyte (specimen courtesy N. Frootko). Fieldwidth = 412µm.

Figure 26. Maxillary **sinus lining bone.** Anorganic preparation showing small resorption lacunae. Fieldwidth = 187µm.

Figure 27. Autopsy of vertebral spongiosa infiltrated with a metastasis from a **carcinoma of the lung.** Very active resorption is indicated by the deep, burrowing type of Howship's lacunae. Fieldwidth = 170µm.

Figures 28 and 29. Autopsy of vertebral spongiosa near to site infiltrated with a secondary of a **carcinoma of the pancreas.** Stimulation of both resorption and formation is seen. Note the new woven bone trabeculae within the inter-trabecular spaces of the original lamellar bone in Fig. 28, and resorption bays in a mineralising front in Fig. 29.
Fieldwidths: Fig 28 = 1390µm. Fig. 29 = 76µm.

with new osteoid. To see the osteoid, therefore, it is necessary to examine LM sections, or to use BS staining for CL in the SEM, or to remove PMMA with a solvent[35].

Osteoporosis

The accelerated loss of bone tissue in women after the menopause is a major problem in all the temperate countries[1,36]. Femoral neck fracture is a common and very serious complication, and death is frequently the eventual outcome. Numerous clinical investigations have clearly demonstrated the importance of the reduction in oestrogen levels after the menopause, inadequate functional loading, reduced dietary calcium intake and lack of exposure to sunlight as some of the most important factors in the etiology of this bone loss.

In our own survey comparing normals with osteoporotic individuals, who had suffered femoral neck fracture, we showed both a reduced trabecular bone volume and an increased relative volume of osteoid, i.e. a degree of histological osteomalacia[37]. The measurement of osteoid using the CL mode in the SEM would certainly make it possible to obtain precise statistical data on this point. However, our methods require that the decision to acquire this information is made in advance of processing the tissue. We cannot merely re-examine existing blocks, because staining with brilliant sulphaflavine (BS) should be done before embedding in PMMA[25] (Figure 2).

So far as we are aware, there are no contra-indications to this procedure: tetracyline lines can still be read in spite of the BS fluorescence and other staining procedures are not excluded. However, it would also be possible to use another embedding medium, for example, glycol methacrylate, to permit the use of a range of post embedding, block surface stains[5].

One of the main parameters in quantifying osteoporosis is evidently the measurement of the bone phase volume. The reduction in the amount of bone in itself makes it difficult to take the trephine core biopsy without damaging the tissue. The trabeculae break, displace, and get bunched together at the periphery of the biopsy, so that this region has to be ignored in quantifying bone - but not in assessing the proportion of osteoid to bone. In the normal procedure, the few trabeculae may be further disadvantaged in sectioning. Simple BSE-SEM based image analysis of the block face is therefore the best way to measure trabecular bone volume (TBV) and surface area well as trabecular thickness (fig. 18). In an unpublished study with I. Bab, we were able to find a good correlation between TBV measured in LM sections and the block face where the TBV was in the normal range (eg. 18-25% Fig 18). However, there was a discrepancy in the values in the lower part of the range: we believe that the SEM based values must be the more reliable.

Primary hyperparathyoidism (PHPT)

Study with R. Weinstein.

High levels of circulating PTH secreted by a parathyroid tumour induce hypercalcaemia and both heightened bone resorption and new bone replacement[10,30,45-48,50-52,54-57,77]. PHPT bone samples show an increased proportion of both mineralising fronts and resorption surfaces (Figs. 19-21). The bone shifts towards the juvenile condition and areas of frank foetal bone formation can be found. However, PHPT is one of a variety of conditions in which some investigators have not implicitly recognised the characteristics of the more immature forms of bone[8,10,53,54,66,77] (Fig 19). This has led to the previously widespread notion of the existence of a process of "osteocytic osteolysis[9,11,13]". In PHPT there may be areas where mineralisation is deficient in the walls of osteocyte lacunae (fig. 19) which were also larger (and more numerous) at the time of the completion. These would be recognised as enlarged lacunae, or lacunae with circumlacunar mineralisation deficiency in the walls of lacunae opened by cutting or fracturing. In areas of old bone removed by resorption in PHPT, it is possible to see that (as in normal bone) osteocyte lacunae display intact mineralised collagen fibres in their walls demonstrating that the osteocytes do not attack the walls of their houses[13] (Fig. 20).

Fluorosis

Study with J. M. Faccini, and S. Teotia

Flouride ingested at excessive levels induces well marked changes in bone tissue, probably due to the decreased solubility of the bone mineral and a degree of secondary hyperparathyroidism[37,40]. We have examined several biopsies from patients from an area in India with endemic fluorosis due to high F levels in the drinking water[37]. The bone volume fraction is increased, and the pattern of

organisation affected (Figs. 22 and 23). There are many areas where the numbers and sizes and distances between osteocyte lacunae all indicate that the bone is foetal or woven in character. i.e this is rapidly formed bone tissue. There is also a higher incidence of circumlacunar mineralisation deficiences so that measurement of lacunae size from BSE images using the Quantimet 720-SEM combination, showed an increased proportion of enlarged mineral phase lacunae.

Paget's disease

Paget's disease of bone is a high bone turnover condition with a patchy localisation[31,58]. It is presently considered that it is caused by an earlier infection by a member of the paramyxo family of viruses. As in other high turnover conditions, we have found a higher incidence of immature forms of bone in Pagetic tissue: i.e. larger, more numerous lacunae, with less well mineralised walls. In cut surfaces, we have found circumlacunar mineralisation deficiencies (Fig. 24) which others have taken as osteocytic osteolysis.

Bone associated with the respiratory system: the auditory ossicles and air sinus lining surfaces . Study with N. Frootko[38].

The condition of the bone in the auditory ossicles presents a stark contrast to the high turnover conditions. They scarcely grow from birth, and there is scarcely any remodelling. We have examined many ossicles removed at post mortem from individuals with no history of specific hearing-related diseases, and at operation for reconstruction of the ossicular chain, mostly necessitated by the long term consequences of chronic inflammatory disease. These studies will be reported in detail elsewhere. We note, however, two special features of these bones. First, as regards osteocytes, there are numerous infilled lacunae with strong suggestive evidence that the residue of the cell itself constitutes the matrix for mineralisation (fig. 25). The bone appears qualitatively rather denser. Secondly, we have seen many instances where resorptive surfaces showed resorption pits which were smaller than the range of sizes we have encountered elsewhere in both normal and pathological bone (Fig. 26). The idea springs to mind, therefore, that this resorption may have been conducted by somewhat smaller, perhaps mononucleate cells. It is certain that the environment of the bone surface of the auditory ossicles is exceptional, compared with most of the skeleton, in that it is just deep to a wet epithelium. Inflammatory cells of all types are therefore found in this vicinity. The literature contains several references to work purporting to demonstrate the ability of macrophages to resorb bone[55,72,75] and we ask whether these might be the cells responsible for this unusual resorption? However, it is (a) not proven that small cells were necessarily involved, since isolated osteoclasts can, on occasion, make many small resorption pits in vitro[43] and (b) also possible that uninucleate, differentiated dedicated osteoclasts were involved. We have also seen this resorption pattern in the bone next to the lining of a maxillary air sinus (Fig. 26).

Metastatic spread of tumours to bone

Several malignancies (e.g. breast, prostate, lung (Fig. 27), pancreas (Figs. 28 and 29)) characteristically metastasise to bone and are associated with a marked hypercalcaemia[57]. Destruction of bone tissue in the vicinity of the tumour tissue can be catastrophic (fig. 27), leading for example, to vertebral collapse. We have examined post mortem vertebral spongy bone samples to determine whether there was any evidence, from the morphology of bone surfaces, to suggest that the bone destruction was mediated by cells other than osteoclasts. In the examples which we studied (and in animal model material of an analogous nature), we have been unable to find any appearances differing from the usual osteoclastic resorption. Thus it would seem that the tumour tissue was not directly involved, but was able, either directly itself, or via the stimulation of lymphocyte activity, to produce a factor which stimulated resorption by recruiting and/or activating otherwise normal osteoclasts[57]. The stimulation of bone resorption is associated with hyperactive bone formation at nearby sites in many cases. This is illustrated by a case of infiltrating carcinoma of pancreas in vertebral trabecular bone in Figs. 28 and 29.
(Bone tumours as such are discussed by Sela[68]).

Discussion

SEM studies in bone pathology could never replace routine LM histology in diagnosis and histomorphometry. We feel, however, that the more detailed study of selected samples in the SEM can aid in understanding the disease process and amplify or confirm LM findings.

We particularly wish to draw attention to the possibility with SEM to examine features which are just too difficult to see with the LM - such as details of the mineralising front, and the pattern of the collagen fibres in the walls of osteocyte lacunae. Indeed, careful study of such features has helped to change current opinion concerning the likelihood of the existence of a particular (patho-) physiological process, osteocyte osteolysis. The possibilities of discovery through 3-D reconstruction should also not be underestimated - both 3-D through stereo viewing and stereo measurement[21,41,43] and also of 3-D via serial grinding and polishing (or micro-milling) through a solid block. Thus we would wish to explore and exploit the potential of reconstructing bone tissue not just in terms of "bone" (e.g. trabecular), but also of whether it is highly mineralised, or normally or poorly mineralised. The organisation of the interfaces between bone phases with different characteristics ought to affect its mechanical properties. So, for example, the ultra-common disease of ageing, osteoporosis, should be re-examined to see whether there are factors other than quantity which might be involved.

Routine SEM is no more expensive and no more

complicated than routine LM. In fact, nowadays, one could almost say that it was both simpler and cheaper, and it is certainly quicker (unless PMMA embedding is involved). The demand for the services of scanning electron microscopy in bone pathology will, however, be controlled by pathologists, and we can only expect a slow development of interest in this field. We may be forgiven for wondering what would be the relative importances of SEM and LM if they had been discovered in reverse order!

Apropos the TSRLM, we commend its use in studying bone remodelling phenomena, and highly recommend it for any studies involving bone implant materials: it is suited because the bone+implant block has only to be cut once. In the case of the TSRLM, it is the limited availability of this microscope which is more likely to restrict the expansion of its use than any appparent complexity; for, as an LM, it does not carry the mystique of electron optics with it to deter the pathologist.

Acknowledgements

Work at UCL Hard Tissue Unit has been supported by grants from the Medical Research Council, The Foundation for Age Research, The Science and Engineering Research Council and the Central Research Fund of the University of London. S.A.R. was supported for 3 years by a post-graduate studentship from the Anatomical Society of Great Britain and Ireland. We are deeply grateful for the interest and collaboration of the many people who have loaned material for the studies reported here, including I. Bab, J. Blenkinsop, J. & D. Birkenhager, B. Boyce, J. M. Faccini, N. Frootko, G. Mechanic, F. Melsen, M. Nimni, R. Steendijk, S. Teotia, R. Weinstein. Sheila J. Jones has helped in innumerable ways. Roy Radcliffe has provided valuable technical assistance, Carl Prescott helped to establish important parts of our equipment and mended our geriatric SEM all too often. Peter Howell made our image analysis system and wrote its software.

References

1 AARON JE, GALLAGHER JC, ANDERSON J, STASIAK L, LONGTON EB, NORDIN BEC, NICHOLSON M (1974) Frequency of osteomalacia and osteoporosis in fractures of the proximal femur. Lancet **1:**785.

2 AMPRINO R, ENGSTROM A (1952) Studies on x-ray absorption and diffraction of bone tissue. Acta Anat. **15:** 1-22.

3 ANDERSON C, DANYLCHUK KD, (1978) Dense mineralised perivascular tubules in osteopetrotic bone. Clin. Orthop. **137:** 265-267

4 AVIOLI LV, TEITELBAUM SL (1976) The renal osteodystrophies. In: The Kidney (Brenner BM, Rector FC, eds), W. B. Saunders, Philadelphia, pp. 1542.

5 BAB I, ASHTON BA, OWEN ME, BOYDE A (1984) Incident light microscopy of surfaces of plastic embedded hard tissues. J.Microsc. **134:** 49-53.

6 BALL J, GARNER A (1966) Mineralisation of woven bone in osteomalacia. J. Pathol. Bact. **91:** 563.

7 BAUD C.A. (1968) Submicroscopic structure and functional aspects of the osteocyte. Clin. Orthop. Rel. Res. **56:** 227-236.

8 BAUD C.A., BOIVIN G. (1978) Effects of hormones on osteocyte function and perilacunar wall structure. Clin. Orthop. Rel. Res. **136:** 270-281.

9 BELANGER L.F. (1969) Osteocytic osteolysis. Calc. Tiss.Res. **4:** 1-12.

10 BERNARD J., MEUNIER P. (1975) L'analyse morphometrique de l'osteolyse periosteocytaire. Son application au diagnostic des hyperparathyroidies. Ann. d'Anat. Path., Paris **20:** 367-380.

11 BOYCE BF, ELDER HY, FELL GS, NICHOLSON WAP, SMITH GD, DEMPSTER DW, GRAY CC, BOYLE IT (1981) Quantitation and localisation of aluminium in human cancellous bone in renal osteodystrophy. Scanning Electron Microsc. 1981; III: 329-337.

12 BOYDE A (1972) SEM studies of bone. In: The Biochemistry and physiology of bone (Bourne GH, ed), 2nd edn, Vol.1. New York: Academic Press, pp. 259-310.

13 BOYDE A (1980) Evidence against osteocytic osyeolysis. Metab. Bone Dis. Rel. Res. **2S:** 239-255.

14 BOYDE A (1984) Methodology of calcified tissue specimen preparation for SEM. In: Methods of Calcified Tissue Preparation (ed Dickson GR), Elsevier, Amsterdam, pp. 251-307.

15 BOYDE A, FRANC F (1980) Converted backscatterred electron imaging for bone morphometry. Metab. Bone Dis. Rel. Res. **2S:** 490-491.

16 BOYDE A, HOBDELL MH (1969) SEM of lamellar bone. Z. Zellforsch. **93:** 213-231.

17 BOYDE A, HOBDELL MH (1969) SEM of primary membrane bone. Z. Zellforsch **99:** 98-108.

18 BOYDE A, HOWELL, PGT, JONES SJ (1974) Measurement of lacunar volume in bone using a stereological grid counting method evolved for the SEM. J Microsc. **101:** 261-266.

19 BOYDE A, JONES SJ (1972) SEM studies of the formation of mineralised tissues. In: Developmental Aspects of Oral Biology (Slavkin HC, Bavetta LA, eds), Academic Press, New York, pp. 243-273

20 BOYDE A, JONES SJ (1974) Preparation of bone and other hard tissue specimens for SEM. In: Principles and techniques of SEM, Vol. 2 (Hayat MA, ed), Van Nostrand Reinhold Co, New York, pp. 123-149.

21 BOYDE A, JONES SJ (1979) Estimation of the size of resorption lacunae in mammalian calcified tissues by SEM photogrammetry. Scanning Electron Microsc. 1979; II: 393-402.

22 BOYDE A, JONES SJ (1983) Backscattered electron imaging of skeletal tissues. Metab. Bone Dis. Rel. Res. 5: 145-150.

23 BOYDE A, JONES SJ (1983) Scanning electron microscopy of cartilage. In: Cartilage 1 (Hall BK, ed), vol. I, Academic Press Inc., USA, pp. 105-148.

24 BOYDE A, PETRAN M, HADRAVSKY M (1983) Tandem scanning reflected light microscopy of internal features in whole bone and tooth samples. J.Microsc. **132:** 1-7.
25 BOYDE A, REID SA (1983) New methods for cathodoluminescence in the SEM. Scanning Electron Microsc. 1983; IV: 1803-1814.
26 BOYDE A, REID SA (1983) Simple collectors for cathodoluminescence in the SEM made from aluminium foil. J.Microsc. **132:** 239-242.
27 BOYDE A, REID SA (1983) Tetracycline cathodoluminescence in bone, dentine and enamel. Histochemistry **77:** 525-533.
28 BOYDE A, REID SA, HOWELL PGT (1983) Stereology of bone using both backscattered electron and cathodoluminescence imaging for the SEM. Beitr. elektronenmikroskop. Direktabb. Oberfl. **16:** 419-430.
29 BOYDE A, SHAPIRO IM (1987) Mineralisation of normal and rachitic chick growth cartilage: relationship between vascular canals, cartilage calcification and osteogenesis. Scanning electron Microsc. 1987: in press.
30 BYERS PD, SMITH R (1971) Quantitative histology of bone in hyperparathyroidism. Its relation to clinical features, x-ray and biochemistry. Qu.J. Med. **40:** 471.
31 CHAPPARD D, ALEXANDRE C, LABORIER JC, ROBERT JM, RIFFAT G (1984) Paget's disease of bone, a scanning electron microscopic study. J. Submicrosc.Cytol. **16:** 341-348.
32 CHOUFOER JH, STEENDIJK R (1979) Distribution of the perilacunar hypomineralised areas in cortical bone from patients with familial hypophosphatemic (vitamin D-resistant) rickets. Calc. Tiss. Int. **27:** 101-104.
33 COURPRON P, GIROUD JM, BRINGUIER JP, MEUNIER P (1974) Histomorphometrie de los spongieux iliaque: Influence des techniques de preparation et de lecture des coupes histologiques sur la determination du volume trabeculaire osseux iliaque. Lyon Med. **232:** 515.
34 DELLING G , and LUEHMANN H. (1980) Correlation of static and dynamic histomorphometric data in secondary hyperparathyroidism. Bone histomorphometry, Third International Workshop. Sun Valley. Metab. Bone Dis. Rel. Res.**2S:** 339-347.
35 DEMPSTER DW, SHANE E, HORBERT W, LINDSAY R (1986) A simple method for correlative light and scanning electron microscopy of human iliac crest bone biopsies: qualitative observations in normal and osteoporotic subjects. J. Bone Min. Res. **1:** 15-21.
36 FACCINI JM, EXTON-SMITH AN, BOYDE A (1976) Disorders of bone and fracture of the femoral neck. The Lancet, May 1976, pp. 1089-1092.
37 FACCINI JM, TEOTIA SPS, (1974) Histopathological assessment of endemic skeletal fluorosis. Calc. Tiss. Res. **16:** 45-57.
38 FROOTKO N, MACONNACHIE E, BOYDE A (1984) The functional state of human incus bone surfaces. J.dent.Res. **63:** 499.
39 FROST HM (1969) Tetracycline-based histological analysis of bone remodeling. Calc. Tiss. Res. **3:** 211-237.
40 HORN V, FRANKE B (1976) Scan microscopic investigation of human industrial fluorosis. Orthop. Z. **114:** 936-945
41 HOWELL PGT, BOYDE A (1984) Three-dimensional analysis of surfaces. In: The Analysis of Organic and Biological Surfaces (ed Echlin P), John Wiley and Sons Inc., New York, pp. 325-349.
42 HOWELL PGT, REID SA (1986) A microcomputer-based system for rapid on-line stereological analysis in the SEM. Scanning **8:** 69-73.
43 JONES SJ, BOYDE A, ALI NN, MACONNACHIE, E (1985) A review of bone cell and substratum interactions. An illustration of the role of scanning electron microscopy. Scanning **7:** 5-24.
44 JOWSEY J, KELLY PJ, RIGGS BL, BIANCO AJ, SCHOLZ DA, GERSHON-COHEN J (1965) Quantitative microradiographic studies of normal and osteoporotic bone. J. Bone Jt. Surg. **47A:** 785-806.
45 KREMPIEN, B (1979) Bone modelling processes at the endosteal surface of human femora. Scanning electron microscopical studies in normal bone aid in renal osteodystrophy. Virchows Arch. (Pathol.Anat.) **382:** 73-88.
46 KREMPIEN B, FRIEDRICH G, GEIGER G, RITZ E (1977) Renal osteodystrophy studies with scanning and transmission electron microscopy. Adv.Exp. Med.Biol. **81:** 493-505.
47 KREMPIEN B, GEIGER G, RITZ E (1975) Alteration of bone tissue structure in secondary hyperparathyroidism. A scanning electron microscopical study. In: Vitamin D and Problems related to Uremic Bone Disease (Norman AW, Schaefer K, Grigoleit H-G, von Herrath D, Ritz E, eds), Walter de Gruyter, Berlin, pp. 157-161.
48 KREMPIEN B, RITZ E, TSCHOPE W (1980) The effect of 1,25 $(OH)_2D3$ on bone mineralisation: Ultrastructural studies in patients with renal osteodystrophy. Contrib.Nephrol. **18:**122-134.
49 LINDENFELSER R, HASSELKUS W, HAUBERT P, KRONERT W (1972) Zur Osteogenesis imperfecta congenita. Rasterelektronenmikroskopische Untersuchungen. Virchows Arch. Abt. B Zellpath. **11:**80-89.
50 LINDENFELSER R, SCHMITT HP, HAUBERT P (1973) Vergleichende rasterelektronenmikroskopische Knochenuntersuchungen bei primaerem und sekundaerem Hyperparathyroidismus. Zur Frage der periosteocytaeren Osteolyse. Virchow's Arch. Abt.A. Path.Anat **360:**141-154.
51 MELSEN F, MOSEKILDE L (1980) Tetracycline based bone morphometry in primary hyperparathyroidism and hyperthyroidism. Metab. Bone Dis.Rel.Res. **2S:** 349-354.
52 MERZ WA, OLAH AJ, SCHENK RK, DAMBACHER MA, GUNAGA J, HAAS HG (1971) Bone remodelling in primary hyperparathyroidism. Preoperative and postoperative studies. Isr. J. Med. Sci. **7;** 494.
53 MEUNIER P, EDOUARD C, COURPRON P, TOUSSAINT F (1974) Morphometric analysis of osteoid in iliac trabecular bone. Methodology. Dynamical significance of the osteoid parameters. In: Vitamin D and Problems related to Uremic Bone Disease (Norman AW, Schaefer K, Grigoleit H-G, von Herrath D, Ritz E, eds), Walter de Gruyter, Berlin, pp. 149-155.
54 MEUNIER P, VIGNON G, BERNARD J, EDOUARD C, COURPRON P, PORTE J (1972) La lecture quantitative de la biopsie osseuse, moyen de diagnostic et d'etude de 106 hyperparathyroidies primitives, secondaires et paraneoplasiques. Revue de

Rhumatisme **39:** 635-644.
55 MUNDY GR, ALTMAN AJ, GONDEK MD, BANDELIN JG (1977) Direct resorption of bone by human monocytes. Science **196:** 1109-1111.
56 MUNDY GR, COVE DH, FISKEN R (1980) Primary hyperparathyroidism: Changes in the pattern of clinical presentation. The Lancet, June 1980, pp. 1317 - 1320.
57 MUNDY GR, IBBOTSON KH, D'SOUZA SM (1985) Tumor products and the hypercalcemia of malignancy. J. Clin. Invest. **76:** 391-394.
58 MUNZENBERG KJ, FLAJS G, ROGGATZ J (1971) Scanning electron microscopy studies on diseased bone structures, especially in Paget's disease of bone. Orthop. Z. **109:** 760-768.
59 ORNOY A, KIM OJ (1977) Scanning electron microscopy findings in osteogenesis imperfecta fetalis. Isr.J.Med.Sci. **13:** 26-32.
60 PETRAN M, HADRAVSKY M, BOYDE A (1985) The tandem scanning reflected light microscope. Scanning **7;** 97-108.
61 PHILLIPS HB, OWEN-JONES S, CHANDLER B (1978) Quantitative histology of bone: a computerised method of measuring the total mineral content of bone. Calc. Tiss Res. **26;** 85-89.
62 REID SA (1987) Micromorphological characterisation of normal human bone surfaces as a function of age. Scanning Electron Microsc. 1987: in press.
63 REID SA (1986) A study of human skeletal maturation using the scanning electron miscroscope. Ph.D Thesis, University of London.
64 REID SA, BOYDE A (1983) SEM and osteogenesis imperfecta. Proc. Symp. Osteogenesis Imperfecta, Oxford, August 29-31, 1983.
65 REID SA, BOYDE A (1986) Changes in the mineral density distribution in human bone with age: image analysis using backscattered electrons in the SEM. J. Bone Min. Res. (in press).
66 RITZ E, KREMPIEN B, RIEDASCH G, KUHN H, HOCKING W, HEUCK F (1971) Dialysis bone disease. Proc. Europ. Dial and Transpl. Assoc. Berlin. p.131. Pitman Medical, London.
67 RITZ E, MEHLS O, KREMPIEN B, GILLI G, UDES H, HARENDZA W (1977) Skeletal Growth in Uremia Adv.Exp.Med.Biol. **81:** 515-531.
68 SELA J (1977) Bone remodeling in pathologic conditions. A scanning electron microscopic study. Calc. Tiss. Res. **23:** 229-234.
69 STEENDIJK R, BOYDE A (1973) SEM observations on bone from patients with hypophospataemic (vitamin D resistant) rickets. Calc. Tiss. Res. **11:** 242-250.
70 STUHLER T, BROCKER W, KAISER G, POPPE H (1979) Fibrous dysplasia in the light of new diagnostic methods. Arch. Orthop. Trauma Surg. **94:** 255-263.
71 TAM CS, HEERSCHE JNM, MURRAY TM, PARSONS JA (1982) Parathyroid hormone stimulates the bone apposition rate independently of its resorptive action: Differential effects of intermittent and continuous administration. Endocrinol. **110;** 506-512.
72 TEITELBAUM SL, KAHN AJ (1980) Mononuclear phagocytes, osteoclasts and bone resorption. Mineral Electrolyte Metab. **3:** 2-9.
73 TEITELBAUM SL, KRAFT WJ, LANG R, AVIOLI LV (1974) Bone collagen aggregation abnormalities in osteogenesis imperfecta. Calc. Tiss. Res. **17:** 75-79.
74 TEITELBAUM SL, NICHOLS SH (1977) Tetracycline-based morphometric analysis of trabecular bone kinetics. In: Bone Histomorphometry (Meunier P, ed), Armour Montagu, Paris, pp. 311-319.
75 TEITELBAUM SL, STEWART CC, KAHN AJ (1979) Rodent peritoneal macrophages as bone resorbing cells. Calc. Tiss. Int. **27:** 255-261.
76 TONNA EA (1972) Electron microscopic evidence of alternating osteocytic-osteoclastic and osteoplastic activity in the perilacunar walls of aging mice. Conn.Tiss. Res. **1:** 221-230.
77 VITTALI PH (1968) Osteocyte activity. Clin. Orthop. Rel. Res. **56:** 213-226.

Discussion with Reviewers

Reviewer I: You have devised a series of beautiful methods for the SEM investigation of bone tissue. Unfortunately, the text fails to fulfil the expectations aroused by the title, which implies it will contain methods of proven utility in diagnosis or planning of treatment. None of the methods described has been adequately validated for diagnostic use.

Authors: We are pleased that the basic flavour of our contribution has been understood and accepted. We are sure that the more widespread adoption of the methods which we have been evolving for many years might lead to some small but significant improvements in understanding basic mechanisms at the tissue structure level. We regret that the title raised unfulfilled expectations in the reviewer: it seems to us that the title should not lead anyone to expect anything in particular, except to find a review of the personal studies of the authors concerning, more or less, the question "What has the SEM got to offer in improving our understanding of bone tissue pathology?". We make no claim or suggestion that the SEM and the methods described here are "validated for diagnostic use". We had hoped that the publication of this MS would be one step down that road, in which we have to overcome the resistance to change due to factors such as:
a) the general suitability of established histopathological routines to satisfy the expectations of the pathologist within the limitations of his training programme.
b) the routine load upon the working pathologist which means that he/she does not have the time to experiment with new methodologies.
c) the fact that the methodologies described here are special to the bone field, and therefore do not have too much general applicability in other areas of soft tissue histopathology.
d) the lack of funding, both for basic researchers whose work is not quite accepted by, or respectable to, the clinical bone field and for clinical bone pathologists who would perhaps like to experiment in these areas but would need a higher proportion of technical back-up.
e) the lack of acceptance of the methods considered here simply because they have not yet been adequately researched, automated and "accepted" by peer pathologists.

We hope that the reviewer will at least accept that the stereological investigation of the amount of bone, fractional bone surface etc., etc., using BSE SEM based study of the block face will be a useful tool in future studies of bone biopsies and autopsies.

Reviewer II: In dealing with clinical material it remains important to provide as much information as possible about the source of the bone. For instance, in the osteogenesis imperfecta specimens, it would have been useful to know the clinical type of patient and whether the bone was taken from near site of previous surgery.

Authors: We are fully well aware of the need to have better documentation from the clinicians who have been kind enough to provide us with access to human material for study. Regrettably,however, we are limited by such information as we are able to obtain.

Reviewer II: R. Smith